

Effect of Coulomb Screening Length on Nuclear Pasta Simulations

P. N. Alcain, P. A. Giménez Molinelli, J. I. Nichols and C. O. Dorso
*Departamento de Física, FCEN, Universidad de Buenos Aires, Núñez, Argentina and
IFIBA-CONICET*

(Dated: June 22, 2022)

We study the role of the effective Coulomb interaction strength and length on the dynamics of nucleons in conditions according to those in a neutron star’s crust. Calculations were made with a semi-classical molecular dynamics model, studying isospin symmetric matter at sub-saturation densities and low temperatures. The electrostatic interaction between protons interaction is included in the form of a screened Coulomb potential in the spirit of the Thomas-Fermi approximation, but the screening length is artificially varied to explore its effect on the formation of the non-homogeneous nuclear structures known as “nuclear pasta”. As the screening length increases, we can see a transition from a one-per-cell pasta regime (due exclusively to finite size effects) to a more appealing multiple pasta per simulation box. This shows qualitative difference in the structure of neutron star matter at low temperatures, and therefore, special caution should be taken when the screening length is estimated for numerical simulations.

PACS numbers: PACS 24.10.Lx, 02.70.Ns, 26.60.Gj, 21.30.Fe

I. INTRODUCTION

At densities and temperatures expected to exist in neutron star crusts ($\rho \lesssim \rho_0$ and $T \lesssim 1.0 \text{ MeV}$, with ρ_0 denoting the normal nuclear density), nucleons form structures that are substantially different from the “normal”, quasi-spherical nuclei we are familiar with. Such structures, which have been dubbed “nuclear pasta”, have been investigated using various models [1–12] which have shown them to be the result of the interplay between nuclear and Coulomb forces in an infinite medium. The structure of the nuclear pasta is expected to play an important role in the study of neutrino opacity in neutron stars [13], neutron star quakes and pulsar glitches [14]. In neutron stars, apart from protons and neutrons, there is an electron gas. This electron gas screens the electrostatic long range proton-proton interaction. This screening effect is often modeled within the Thomas-Fermi approximation, according to which, the interaction between protons is a Yukawa-like potential with a screening length λ :

$$V_{TF}(r) = q^2 \frac{e^{-r/\lambda}}{r}$$

According to QFT calculations [15, pp. 175-180], the screening length is $\lambda \approx 100 \text{ fm}$. For numerical simulations, such a long range interaction poses a problem since, to perform correct particle-based simulations, the simulation domain (or cell) should be much larger than the length of the interaction potentials [16]. Using the correct value for λ would then require working with $\mathcal{O}(10^6)$ particles and it would be computationally very exhaustive. Facing this issue, pioneering authors [13, 17] decided to work with a much smaller $\lambda = 10 \text{ fm}$, hoping to retain the main qualitative phenomenological aspects of the system (competing interactions of different length) but with smaller systems. Even if they were indeed capable of producing “pasta-like” structures, the particular

choice of the value for the screening length was arbitrary and based almost solely on computational details. Notably, this particular value of the screening length was used by every author using a screened Coulomb potential for particle-based simulations ever since [7, 12, 13]. This paper will work on studying to which extent this arbitrary choice is physically relevant, expanding previous works.

The role of the length of the screening has been narrowly explored by several authors in other models. For example, in a 2003 investigation [11], the screening effect of an electron gas on cold nuclear structures was investigated using a static liquid-drop model, and it was found that main effect of the gas screening was to extend the range of densities where bubbles and clusters appear and to reduce the range of stability of homogeneous phases. While the screening was found to be of minor importance, the study, being static, didn’t include any spatial or dynamical effect. Another 2005 study [18] used a density functional method to investigate charge screening on nuclear structures at sub-nuclear densities but still at zero temperature; in particular, cases with and without screening were directly compared. The main results of the study were nucleon density profiles used to quantify the spatial rearrangement of the proton and electron charge densities. Once again, it was found that the density region in which the pasta exists becomes broader when the Coulomb screening is taken into account, mainly due to the rearrangement of the protons; the authors remark the importance of extending such study to finite temperatures and with dynamical models.

More recently, some works [19, 20] began studying the effect that Coulomb interaction has on the pasta formation using dynamical models. The main findings are that artificial one-per-cell pasta (*pseudo-pasta*) could exist even when Coulomb interaction was removed, and that they exist due to periodic boundary conditions and

finite size [21].

In a previous study, we showed that a combination of classical molecular dynamics, fragment recognition algorithms and a set of topological tools [12] was very effective in the study of the pasta structures. In particular, we showed that topological observables can be used to classify the different structures into recognizable patterns; this allows for cross-model comparison between structures obtained with different approaches and to a quantifiable analysis of the effect the nuclear and Coulomb energy have on the pasta formation and properties. We will study the extent to which the screening length λ affects the morphology of the ground states at zero temperature of nuclear pasta. To this effect, semi-classical molecular dynamic simulations with a screened Coulomb potential and values of λ from 0 to 50 fm were performed. The model used is described in section II, and in section II A numerical aspects of the Coulomb model used are discussed. Topological tools were used to quantitatively analyse the effect the nuclear and Coulomb energies have on the pasta formation and its properties are introduced in section II C. Results are presented and discussed in section III.

II. CLASSICAL MOLECULAR DYNAMICS MODEL

The model used here was and developed to study nuclear reactions from a semi-classical, particle-based point of view [22]. The justification for using this model in stellar crust environments was presented elsewhere [12], here we simply mention some basic ingredients of the model.

The classical molecular dynamics model *CMD*, as introduced in [23], is retrofitted with cluster recognition algorithms and a plethora of analysis tools. It has been successfully used in heavy-ion reaction studies to help understand experimental data [24], identify phase transitions signals and other critical phenomena [25–28], explore the caloric curve [29, 30] and isoscaling [31, 32]. Synoptically, *CMD* uses two two-body potentials to describe the motion of nucleons by solving their classical equations of motion. The potentials, developed phenomenologically by Pandharipande [22], are:

$$\begin{aligned} V_{np}(r) &= v_r \exp(-\mu_r r)/r - v_a \exp(-\mu_a r)/r \\ V_{nn}(r) &= v_0 \exp(-\mu_0 r)/r \end{aligned}$$

where V_{np} is the potential between a neutron and a proton, and V_{nn} is the repulsive interaction between either *nn* or *pp*. The cutoff radius is $r_c = 5.4$ fm and for $r > r_c$ both potentials are set to zero. The Yukawa parameters μ_r , μ_a and μ_0 were determined to yield an equilibrium density of $\rho_0 = 0.16 \text{ fm}^{-3}$, a binding energy $E(\rho_0) = 16 \text{ MeV/nucleon}$ and a compressibility of 250 MeV [22].

The main advantage of the *CMD* model is the possibility of knowing the position and momentum of all

particles at all times. This allows the study of the structure of the nuclear medium from a particle-wise point of view. The output of *CMD*, namely, the time evolution of the particles in (\mathbf{r}, \mathbf{p}) , can be used as input in any of the several cluster recognition algorithms that some of us have designed for the study of nuclear reactions [33–35].

As explained elsewhere [12, 36, 37], the lack of quantum effects, such as Pauli blocking, –perhaps the only serious caveat in classical models– ceases to be relevant in conditions of high density and temperature (such as in heavy-ion reactions) or in the low-density and low-temperature stellar environments, when momentum transfer between particles ceases to be important.

To simulate an infinite medium, systems with thousands of nucleons were constructed using *CMD* under periodic boundary conditions. Cases symmetric in isospin (i.e. with $x = Z/A = 0.5$, 2500 protons and 2500 neutrons) were constructed in cubical boxes with sizes adjusted to have densities between $\rho = 0.005 \text{ fm}^{-3} \leq \rho \leq 0.08$. Although in the actual neutron stars the proton fraction is low ($x < 0.5$), we chose to work with symmetric matter because that way we could study the Coulomb term without having a symmetry term in the energy.

A. Coulomb interaction in the Model

To take into account the Coulomb interaction, which is formally of infinite range, in molecular dynamics simulation under periodic boundary conditions, it is necessary to use some approximation. The two most common approaches are the Thomas-Fermi screened Coulomb potential (used with various nuclear models, e.g., in *QMD* [7], *CMD* [12] and *SSP* [13]) and the Ewald summation procedure [38]. Theoretical estimations for the screening length λ are $\lambda \sim 100$ fm, but in the previously mentioned works, due to computational limitations, a value of $\lambda = 10$ fm was chosen. Our goal on this work is to understand the effect this *a priori* arbitrary choice has on the properties of the ground states of Neutron Star Matter within the framework of *CMD*.

In this work, we used values of λ ranging from $\lambda = 0$ fm (formally, no Coulomb interaction) and $\lambda = 20$ fm, for densities $\rho = \{0.005 \text{ fm}^{-3}, 0.03 \text{ fm}^{-3}, 0.05 \text{ fm}^{-3}, 0.08 \text{ fm}^{-3}\}$, and the cut-off length was chosen at $r_c = \lambda$. In particular for $\rho = 0.005 \text{ fm}^{-3}$, where “gnocchi” are formed, we extended the analysis to $\lambda = 30$ fm and $\lambda = 50$ fm to perform a quantitative analysis on the physical properties of the clusters.

B. Simulation procedure

The trajectories of the nucleons are then governed by the Pandharipande and the screened Coulomb potentials. The nuclear system is cooled from $T = 1.6 \text{ MeV}$ to $T = 0.001 \text{ MeV}$ using isothermal molecular dynamics with the

Nosé-Hoover thermostat procedure [40], in the LAMMPS package [41]. Systems are cooled in small temperature steps ($\Delta T \approx 0.02$), decreasing the temperature once both the energy and the temperature are stable.

C. Analysis tools

The first of the analysis tools used is the pair correlation function, $g(r)$, which gives information about the spatial ordering of the nuclear medium. In the previous study, $g(r)$ showed that nucleons in clusters have an inter-particle distance of about 1.8 fm at all studied densities for $\lambda = 10$ fm. It is interesting to know if the nearest neighbor distance changes with the screening length.

Beyond local measures, the shapes of nuclear structures can be characterized by a set of morphological and topological observables: their volume, surface area, mean curvature, and Euler characteristic χ . These four objects comprise the ‘‘Minkowski functionals’’ and completely describe all morphological and topological properties of any three-dimensional object [39]. The computation of the mean curvature and χ can be accomplished through the Michielsen–De Raed algorithm but requires the mapping of the nuclear clusters into a polyhedra, procedure described in [12].

In [12] it was shown that generic structures, such as ‘‘gnocchi’’, ‘‘spaghetti’’, ‘‘lasagna’’ and ‘‘crossed-lasagnas’’ or ‘‘jungle gym’’ and their inverse structures (with voids replacing particles and vice-versa), all have well defined and distinct values of the mean curvature and χ with magnitudes dictated by the overall size of the structure, i.e. by the number of particles used. For structures with near-zero Euler number, which signal spaghetti, lasagna and their anti-structures, the values of the Minkowski functionals are sensitive to the choice of two parameters: the size given to each particle and the size of the cells in which we partition the space. This classification is shown in Table I.

TABLE I: Classification Curvature - Euler

	Curvature < 0	Curvature ~ 0	Curvature > 0
Euler > 0	Anti-Gnocchi		Gnocchi
Euler ~ 0	Anti-Spaghetti	Lasagna	Spaghetti
Euler < 0	Anti-Jungle Gym		Jungle Gym

III. RESULTS AND DISCUSSION

As observed in previous works [19, 20], in absence of any Coulomb interaction (what would be equivalent to $\lambda = 0$), pasta-like structures can be seen, although only one per cell. These *pseudo-pastas* are also shaped in spheres, rods, slabs, anti-rods and anti-spheres, just like the pasta with Coulomb interaction. The main difference

is that, without the Coulomb interaction, we find always one structure per cell, giving the hint that its structure is related to the periodic boundary condition imposed on the box. The *pseudo-pasta* exists due to finite size effects and, if the box was not to exist, the solution would be an infinite droplet. We notice, however, that when there is Coulomb interaction, the competition between opposing interactions gives rise to a characteristic length. At sub-saturation densities, this competition is responsible for the pasta phases, and in the limit of very-low densities (and no screening) it shapes the nuclei we are used to.

By increasing the value of λ from 0 to 20 fm we aim to explore the transition from artificial *one-per-cell* pasta, to more realistic situations with more than one structure per cell. Moreover, this enables us to assess the physical implications of the arbitrary and traditional $\lambda = 10$ fm value.

A. ‘‘Critical’’ Screening Length

A first approach to analyze the nature of the pasta obtained is given by taking a quick glance at the pressure of the different configurations.

The pressure is computed by the virial formula

$$P = \frac{N k_B T}{V} + \frac{1}{3} \frac{\sum_i^N \mathbf{r}_i \cdot \mathbf{F}_i}{V}$$

where N is the number of nucleons in the system and \mathbf{F} the force exerted upon each nucleon. The terms in the virial formula apply only to the interactions specific to the model, not contemplating the electron gas pressure. This pressure is not to be mistaken with the pressure expected in neutron star crusts, since electrons should be considered explicitly in order to calculate it correctly, it is merely a test of the mechanical stability of the configurations obtained within this model. In figure 1, we see that for all $\lambda < 10$ fm the pressure is negative.

The negative pressure is a signal that the non-homogeneous structures found are artificial and that the structures found can only exist under periodic boundary conditions (see [19, 21]). This may be better understood by picturing the primitive cell of the simulation as being under the stress caused by its periodic replicas. This means that for such small screening lengths the overall effective interaction is mostly attractive and periodic boundary conditions are still playing a major role in shaping the ground state.

For $\lambda > 10$ fm the pressure becomes positive, meaning that the structures formed in these configurations are not only due to periodic boundary conditions, but Coulomb interaction is beginning to play its intended role. The configurations for these values of λ indeed show density fluctuations of length smaller than the size of the cell, which can only be attributed to the coulomb-nuclear competition. However, the morphology of the structures, as characterized by the topological measures described in section II C, changes drastically with λ .

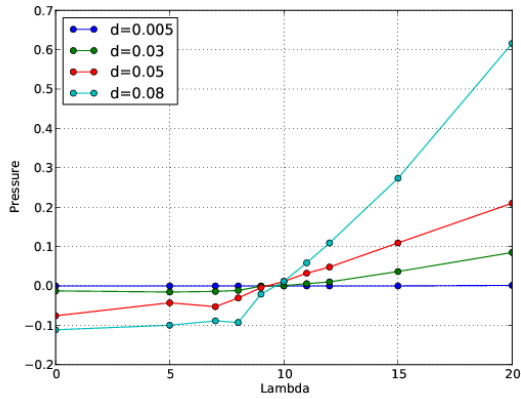


FIG. 1: Pressure as a function of λ for different densities. We see that for $\lambda < 10$ fm, the pressure is negative, implying that periodic boundary conditions are affecting the morphology of the solution.

In order to classify the low temperature ($T = 0.001$ MeV) structures for each value of λ , we study their morphology with the analysis tools for the spatial distribution of the particles; namely, the Minkowski functionals. In figures 2 we can see the surface, curvature and Euler number for the ground states, and their dependence on λ for different densities.

As stated in table I, we expect *lasagna* and *spaghetti* to have an Euler number $\chi = 0$. In the *gnocchi* case, however, each one of them contributes with $\chi_{gn} = 2$. This means that the Euler number of the whole system will be $\chi = 2 \cdot N_{gn}$. As the configurations break up into multiple structures per cell with increasing λ , we expect the surface to increase as well. As for the curvature, the behavior described in table I (positive for *spaghetti* and *gnocchi*, zero for *lasagna* and negative for *tunnel*) is only observed for $\lambda = 20$ fm. Between $\lambda = 7$ fm and $\lambda = 10$ fm all three of the Minkowski functionals change drastically before reaching well defined values. This indicates that there is a transition regime where the structures cannot be described as any of the traditional pasta. For this model of nuclear interaction and Coulomb treatment, it seems the usual $\lambda = 10$ fm value is actually too small.

B. One vs Many

To better understand how the ground state at low temperatures differ on the transition regime from without Coulomb interaction to the $\lambda = 20$ fm screening length, we show in figure 3 visual representations of the results obtained at a set of chosen densities, both with $\lambda = 0$ and $\lambda = 20$ fm.

As an example, we show the pair distribution function, $g(r)$, for $\rho = 0.05 \text{ fm}^{-3}$ in figure 4. In it we see that the first peaks of the distribution remain on the same distances of $r = 1.7$ fm, 1.9 fm. This shows that the short

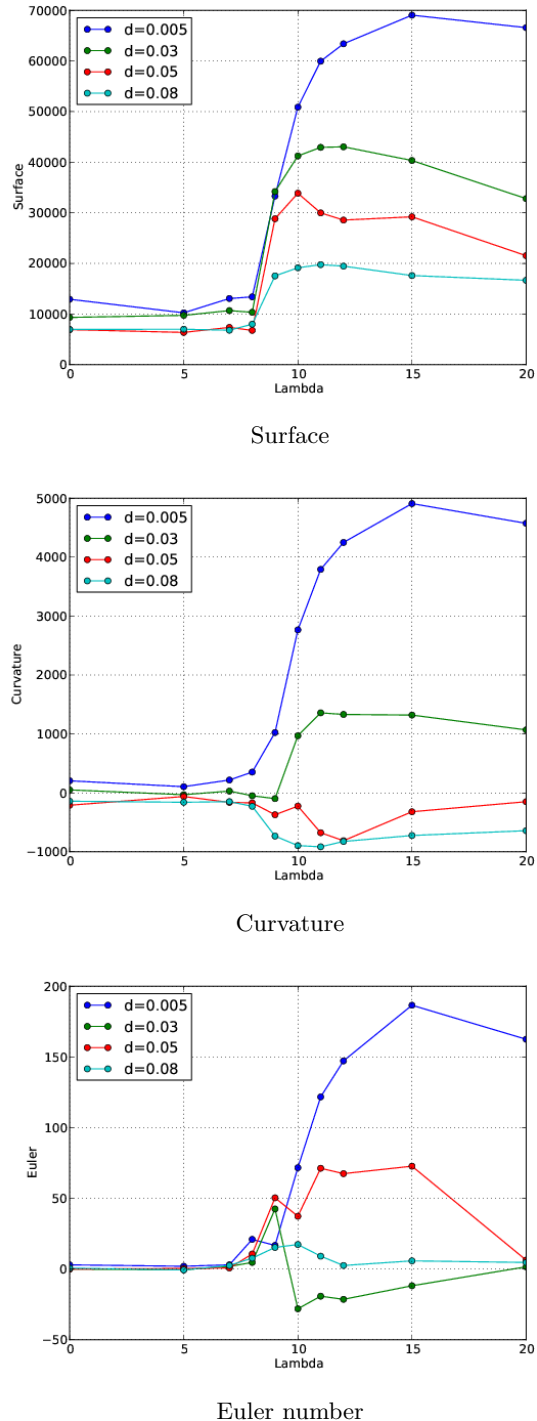


FIG. 2: Minkowski functionals dependence with λ . We can see that there is a transition regime between $\lambda = 7$ fm and $\lambda = 15$ fm, where the Minkowski functionals are changing.

range structure is governed by the nuclear potential even at $\lambda = 20$ fm, which is evident simply by comparing the orders of magnitude of V_{n-n} and V_{Coulomb} at such short

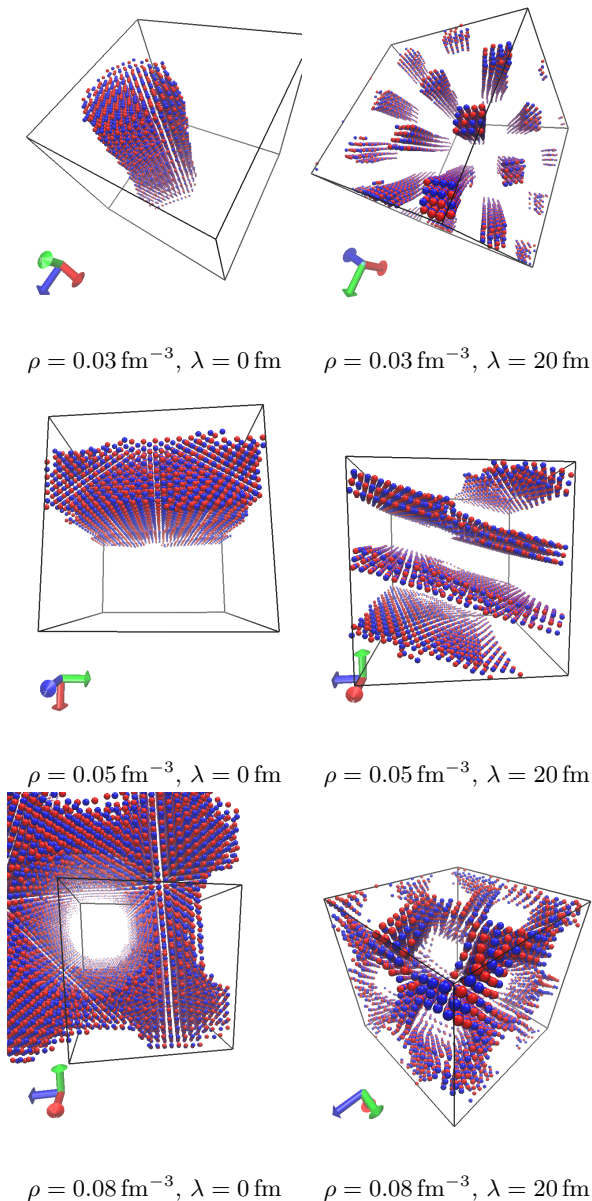


FIG. 3: Difference between pasta with and without Coulomb interaction. We can see that the Coulomb interaction splits up the pasta, converting one structure per cell to multiple structures per cell.

ranges.

When increasing from $\lambda = 15 \text{ fm}$ to $\lambda = 20 \text{ fm}$ at $\rho = 0.005 \text{ fm}^{-3}$, although qualitatively we see the same behavior (both show *gnocchi*), the average size of cluster is different for these two values of screening length. This implies that the number of clusters is different, hence the difference observed in the Minkowski functionals. To study this result further, we plot the “gnocchi” size as a function of λ in figure 5. We see that, when we consider the standard deviation in the mass distribution, it remains unchanged for $\lambda \geq 20 \text{ fm}$. The average relative

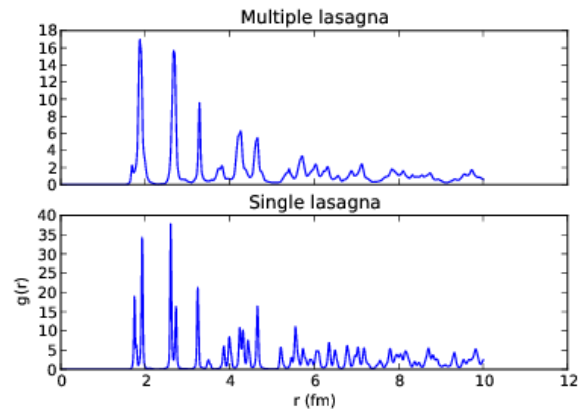


FIG. 4: Examples of the radial correlation function for $\rho = 0.05 \text{ fm}^{-3}$ and two screening lengths: $\lambda = 20 \text{ fm}$ (top panel) and $\lambda = 0 \text{ fm}$ (lower panel). Please notice the difference in the y-scales of the graphs.

error on this graph is $e \approx 8\%$.

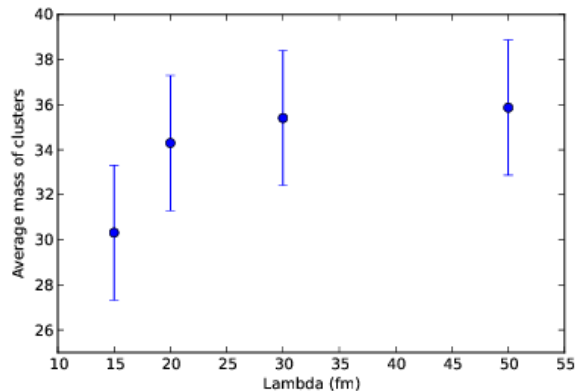


FIG. 5: Average size of nuclei depending on the screening length. We can see that, when considered the standard deviation, the mass remains the same.

We can see here, however, that though the pasta structures without Coulomb is indeed one of the known pasta structures, once we turn on the Coulomb interaction (by making $\lambda \neq 0$) the original $\lambda = 0$ *pseudo-pasta* splits up: from one structure per cell to multiple structures per cell. For intermediate to low values of $\lambda < 20 \text{ fm}$, the effect of the periodic boundary conditions is still observable for some densities and more exotic structures which can be confused with “true” pasta may exist.

C. The Transition Regime

We now turn to analyze the structures found in the transition regime.

We take, as an example, the lowest density ($\rho = 0.005 \text{ fm}^{-3}$). As can be seen in figure 6, for $\lambda = 0$ only one droplet is formed, as expected. For $\lambda = 10 \text{ fm}$, we can see that many *gnocchi* exist, but some of them stick to their neighbors forming lumps of different sizes. Although Coulomb interaction is now strong enough to break the one-pasta found with $\lambda = 0$ into many, the resulting droplets are not fully fledged *gnocchi* that can be arranged in a regular lattice such as those for $\lambda = 20 \text{ fm}$.

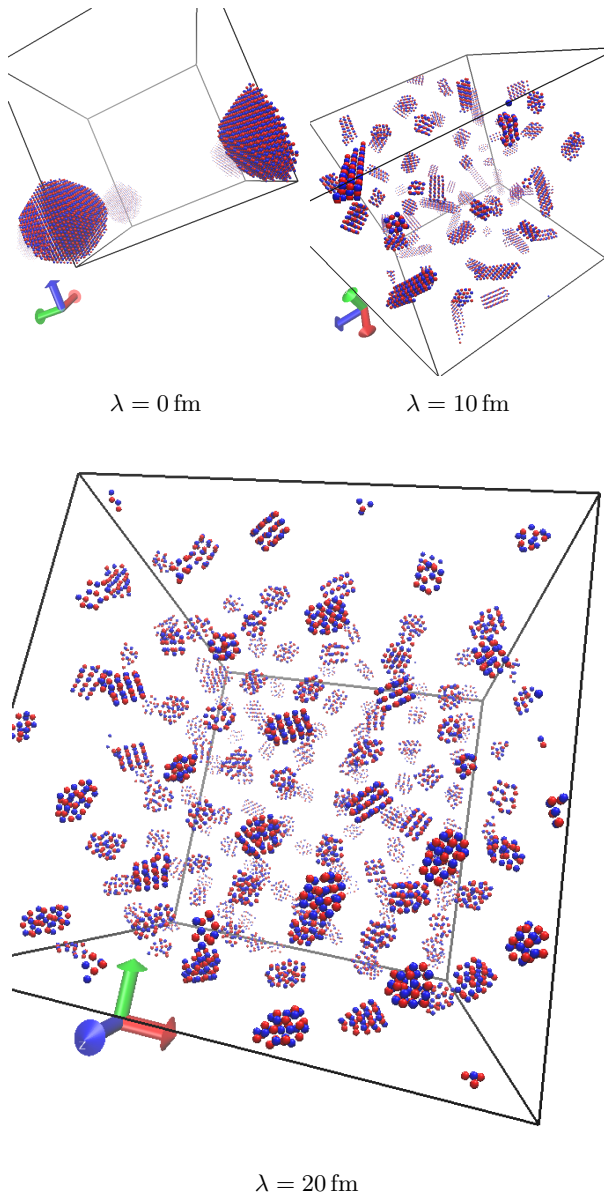


FIG. 6: Different structures got while varying the λ parameter, for $\rho = 0.005 \text{ fm}^{-3}$. In the transition regime, we find, at $\lambda = 10 \text{ fm}$, that the structure breaks down to many *short-spaghetti*-like parts.

IV. DISCUSSION AND CONCLUDING REMARKS

The effect of the screening length of the Coulomb interaction in simulations of neutron star matter was studied at densities comparable to that of neutron star crusts. Subsequently along the literature we can find that the value of the screening length in the Thomas-Fermi approximation is $\lambda \approx 100 \text{ fm}$. For particle-based simulations, due to computational limitations this value was historically and arbitrarily reduced to $\lambda \approx 10 \text{ fm}$. This was done expecting to maintain the basic phenomenology when simulating small systems. We found, though, that there is a critical screening length λ_c at which the structure of the ground state drastically changes. For Pandharipande potential it lies between 10 fm and 15 fm (depending on the density). For $\lambda < \lambda_c$, the Coulomb interaction is barely acting and the non-homogeneous structures emerging from the simulations are due to finite size effects, as made evident from the negative pressure of such structures and the fact that there is only one structure per cell. For $\lambda > \lambda_c$ the pressure becomes positive and the systems present density fluctuations at a scale smaller than that of the cell, but not well shaped. This transition regime is characterized by large fluctuations in the surface, curvature and Euler characteristic χ of the structures. It is only for $\lambda = 20 \text{ fm}$ that the morphology of the structures formed stabilize and cease to depend on λ . Moreover, the structures in this regime are the usual pasta phases.

Because of this, we believe extreme caution should be taken when choosing an arbitrary value for λ , since even though some results at $\lambda = 10 \text{ fm}$ can look like the expected pasta, the results obtained for that particular choice of λ may be quite different from those in the true Thomas-Fermi approximation. In conclusion, we find the choice of a good value for λ that is computationally manageable and can still adequately recover the physics of the Thomas-Fermi approximation is no trivial task, and a rigorous study needs to be done prior to the choice of the value. A good value for λ must lie in the $\lambda > \lambda_c$ region which is bound to be dependent on the model used for the nuclear interaction.

ACKNOWLEDGMENTS

C.O.D. is supported by CONICET Grant PIP0871, P.G.M., J.I.N and P.N.A. by a CONICET scholarship. The three-dimensional figures were prepared using the software *Visual Molecular Dynamics* [42].

[1] D. G. Ravenhall, C. J. Pethick and J. R. Wilson, Phys. Rev. Lett. **50**, 2066 (1983).

[2] M. Hashimoto, H. Seki and M. Yamada, Prog. Theor.

- Phys. **71**, 320 (1984).
- [3] R. D. Williams and S. E. Koonin, Nucl. Phys. **A435**, 844 (1985).
- [4] K. Oyamatsu, Nucl. Phys. **A561**, 431 (1993).
- [5] C. P. Lorenz, D. G. Ravenhall and C. J. Pethick, Phys. Rev. Lett. **70**, 379 (1993).
- [6] K. S. Cheng, C. C. Yao and Z. G. Dai, Phys. Rev. **C55**, 2092 (1997).
- [7] T. Maruyama, K. Niita, K. Oyamatsu, T. Maruyama, S. Chiba and A. Iwamoto, Phys. Rev. **C57**, 655 (1998).
- [8] T. Kido, Toshiki Maruyama, K. Niita and S. Chiba, Nucl. Phys. **A663-664**, 877 (2000).
- [9] G. Watanabe, K. Iida and K. Sato, Nucl. Phys. **A676**, 445 (2000).
- [10] G. Watanabe, K. Sato, K. Yasuoka and T. Ebisuzaki, Phys. Rev. **C66**, 012801 (2002).
- [11] G. Watanabe and K. Iida, Phys. Rev. **C68**, 045801 (2003).
- [12] C.O. Dorso, P.A. Giménez Molinelli and J.A. López, in “Neutron Star Crust”, Eds. C.A. Bertulani and J. Piekarewicz, in print, Nova Science Publishers, Inc. (2012).
- [13] C.J. Horowitz, M.A. Perez-Garcia, and J. Piekarewicz, Phys. Rev. **C69**, 045804 (2004).
- [14] Y. Mochizuki and T. Izuyama, Astrophys. J. **440**, 263 (1995).
- [15] A. L. Fetter and J. D. Wallecka, *Quantum Theory of Many-Particle Systems*, McGraw-Hill (1971)
- [16] D. Frenkel and B. Smit, “Understanding Molecular Simulations”, 2nd Ed., Academic Press (2002).
- [17] Maruyama, Watanabe and Chiba, Prog. Theor. Exp. Phys. **2012**, 1, (2012)
- [18] T. Maruyama, T. Tatsumi, D.N. Voskresensky, T. Tanigawa and S. Chiba, Phys. Rev. **C72**, 015802 (2005).
- [19] C. O. Dorso, P. A. Giménez Molinelli, J. I. Nichols, J. A. López, <http://arxiv.org/abs/1211.5582>
- [20] A. S. Schneider, C. J. Horowitz, J. Hughto, D. K. Berry, <http://arxiv.org/abs/1307.1678>
- [21] Binder, K. et al, Am. J. Phys. **80**, 1099
- [22] A. Vicentini, G. Jacucci and V. R. Pandharipande, Phys. Rev. **C31**, 1783 (1985); R. J. Lenk and V. R. Pandharipande, Phys. Rev. **C34**, 177 (1986); R.J. Lenk, T.J. Schlagel and V. R. Pandharipande, Phys. Rev. **C42**, 372 (1990).
- [23] A. Barrañón, C.O. Dorso, J.A. López and J. Morales, Rev. Mex. Fís. **45**, 110 (1999).
- [24] A. Chernomoretz, L. Gingras, Y. Larochelle, L. Beaulieu, R. Roy, C. St-Pierre and C. O. Dorso, Phys. Rev. **C65**, 054613 (2002).
- [25] A. Barrañón, C.O. Dorso and J.A. López, Rev. Mex. Fís. **47-Sup. 2**, 93 (2001).
- [26] A. Barrañón, C.O. Dorso, and J.A. López, Nuclear Phys. **A791**, 222 (2007).
- [27] A. Barrañón, R. Cárdenas, C.O. Dorso, and J.A. López, Heavy Ion Phys. **17**, 59 (2003).
- [28] C.O. Dorso and J.A. López, Phys. Rev. **C64**, 027602 (2001).
- [29] A. Barrañón, J. Escamilla Roa and J.A. López, Braz. J. Phys., **34-3A**, 904 (2004).
- [30] A. Barrañón, J. Escamilla Roa and J.A. López, Phys. Rev. **C69**, 014601 (2004).
- [31] C.O. Dorso, C.R. Escudero, M. Ison and J.A. López, Phys. Rev. **C73**, 044601 (2006).
- [32] C.O. Dorso, P.A. Giménez Molinelli and J.A. López, J. Phys. G: Nucl. Part. Phys. **38**, 115101 (2011); *ibid*, Rev. Mex. Phys., **S 57 (1)**, 14 (2011).
- [33] C.O. Dorso and J. Aichelin, Phys. Lett. **B345**, 197 (1995).
- [34] A. Strachan and C.O. Dorso, Phys. Rev. **C55**, 775 (1997); *ibid*, Phys. Rev. **C56**, 995 (1997).
- [35] C.O. Dorso and J. Randrup, Phys. Lett. **B301**, 328 (1993).
- [36] J.A. López and C.O. Dorso, Lecture Notes on Phase Transformations in Nuclear Matter, World Scientific, Hackensack, NJ, USA, ISBN 978-981-02-4007-3 (2000).
- [37] J. Taruna, “The physics of compact stars”, Ph.D. Thesis, Florida State University, AAT 3321532 (2008).
- [38] G. Watanabe, K. Sato, K. Yasuoka and T. Ebisuzaki, Phys. Rev. **C68**, 035806 (2003)
- [39] K. Michielsen and H. De Raedt, Phys. Reports **347**, 461 (2001).
- [40] S. Nose, J. Chem. Phys. **81**, 511 (1984)
- [41] S. Plimpton, J. Comp. Phys., **117**, 1-19 (1995)
- [42] Humphrey, W., Dalke, A. and Schulten, K., ‘VMD - Visual Molecular Dynamics’, J. Molec. Graphics **14.1**, 33 (1996).